Proceedings

Geohazards

Engineering Conferences International *Year* 2006

Instability in Soft Sensitive Clays

V. Thakur[*] G. Grimstad[†]

S. Nordal[‡]

[*]ICG and Geotechnical Division, NTNU, vikas.thakur@ntnu.no

[†]ICG and Geotechnical Division, NTNU, gustav.grimstad@ntnu.no

[‡]Division of Geotechnical Engineering, Norwegian University of Science and Technology, steinar.nordal@ntnu.no

Instability in Soft Sensitive Clays

V. Thakur[1], G.Grimstad[2] and S. Nordal[3]

ICG and Geotechnical Division, NTNU, Trondheim, Høgskoleringen 7a, Gløshaugen, Trondheim, NO-7491, Norway; PH (+47) 73 59 69 70; FAX (47) 73 59 46 09;
e-mail : vikas.thakur@ntnu.no[1] gustav.grimstad@ntnu.no[2] steinar.nordal@ntnu.no[3]

Abstract

Soft sensitive clays like quick clays are well known in Scandinavia and in some regions in Canada. The salt pore water of these marine clays has been leached out since last glaciations and left a brittle mineral structure. Slides in quick clays can be extremely disastrous, as in Verdal, Norway in 1893 or Rissa in 1978. The slides may be initiated by local overloading, river erosion or similar and can escalate in size in a retrogressive manner in which large volumes of clay finally may liquefy.

Norwegian quick clay has a very low permeability and hence pore water pressure becomes a crucial parameter that can affect the stability of material. Failure in quick clay (with a post-peak strain softening behavior) is often associated with the development of shear bands, i.e. narrow zones of localized deformation, and the failure loads depend on the thickness of these shear bands. Plane strain compression tests were performed, at laboratory 3S, Grenoble France, to observe the formation and propagation of shear bands during undrained shearing. Biaxial plane strain tests were performed in quick clay having different sensitivity and local pore pressure variation throughout the test was monitored. Image analysis is done to detect shear band thickness and mode of failure.

Further, usefulness of shear band analyses in landslide calculation using finite elements and consequence of such failure is also discussed numerically. A stability analysis of a quick clay slope is made to illustrate the progressive failure mechanism.

Introduction

Soft sensitive clays, also termed quick clays, usually exhibit sensitivity greater than 30 and have remoulded shear strength less than 0.5 kPa. Here, sensitivity is defined as a ratio of undisturbed undrained shear strength to the remoulded undrained shear strength of the material. Landslide in soft sensitive clays may be resulted due to drastic reduction in shear resistance. This may happen due to local overloading, river erosion or similar and can escalate in size in a retrogressive manner in which large volumes of clay finally may liquefy. In highly sensitive clays, therefore, it is not just the risk of a slope failure that is of concern, but also the area that is affected by retrogressive sliding.

In short, landslide phenomena can be decomposed into three distinct phases: initiation or triggering, the slide progression, which includes debris flow, and finally the impact of the slide with natural or human made obstacles. This study only covers with the first two phases.

Triggering and propagation of progressive failure is often associated with the formation of shear bands, i.e. narrow zones of localized deformation, and the failure loads depend on the thickness of these shear bands. Hence thickness and orientation of shear band becomes crucial parameters while analyzing slope failure in soft sensitive clays.

The initial part of the paper provides a brief description of an experimental investigation of measured shear band thickness in Norwegian quick clay using a plane strain biaxial apparatus available at Laboratoire 3S, Grenoble, France. Collaboration between Laboratoire 3S and NTNU Geoteknikk together with ICG was established to pursue the experimental work.

The next part of the paper demonstrates regularization of strain localization in soft sensitive clays using the Hardening Soil model available in the fine element code Plaxis. Finally, a progressive failure mechanism in a slope stability problem is studied using the finite element (FE) method.

Experimental investigation of instability in quick clay

Plane strain compression tests on Norwegian quick clay were performed in 2005 in a plane strain compression device at the Laboratoire 3S of Grenoble. The apparatus was originally developed in Grenoble by Desrues (1984) and later modified by Hammad (1991). The design of this biaxial apparatus shares concepts with those developed by Vardoulakis & Goldscheider (1981) and by Drescher et al. (1990), in that the biaxial apparatus was designed to allow for free shear band formation in a soil specimen.

A 34 mm thick prismatic quick clay specimen, surrounded by a latex membrane, is mounted between two rigid walls inducing plane strain conditions. The initial height and width of the specimen (in the plane of deformation) were 120 mm and 60 mm, respectively. The side walls are 50 mm thick glass plates which allow photographs to be taken of the in-plane deformation of a specimen during the test. All surfaces in contact with the specimen are lubricated with silicone grease to minimize friction.

Together with the measurement of boundary forces and deformations, a Digital camera was used to capture non-homogeneous deformation throughout a test. Systematic analysis of photographs of the deforming specimen allowed for measuring deformations and determining strain fields throughout the test, that is: prior to, at, and after the onset of strain localization. Moreover, the stereoscopic view of successive photographs allowed for measuring shear band orientation with an accuracy of ± 1°.

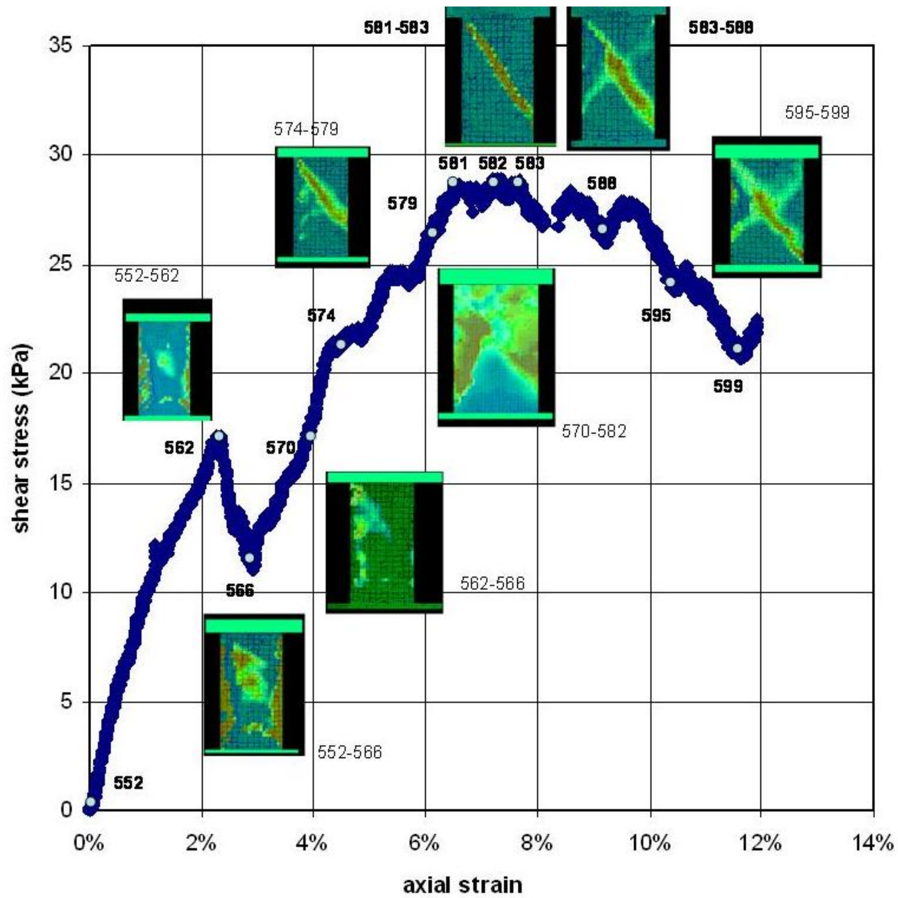

Figure1. Plane strain biaxial stress strain relationship for the Norwegian Quick clay

Figure 1 shows a stress strain response obtained from the laboratory biaxial plane strain test. In this test, the obtained maximum shear stress is 28 kPa at 7% axial strain, which is a high value for a quick clay. Image analyses has been carried out using a Particle Image Velocimetry (PIV) technique and results are given in Figure 1. For biaxial tests with a low rate (as in this case; 0.36%/hr), shear band emerges well before the peak (refer 574-579). This may happen due to the heterogeneity in the specimen. A unique shear band is observed near to the peak (refer 581-583) while a secondary shear band emerged in a perpendicular direction (refer 583-588) once the peak is passed. Finally, the specimen is separated into multiple blocks (refer 595-599) separated by the shear bands, and the shear resistance is reduced. Note that the PIV pictures shown above the curve in Figure 1 show incremental shear strains not total shear strains. The PIV pictures given below the curve show total shear strain plots (refer 570-582) etc., which apparently are not so well suited to study the kinematics of the deforming body. The incremental shear strain are additional strains that develop within a certain short time interval neglecting previous strains. Obviously incremental shear strains must be used to detect shear banding at the different load levels. For the results shown in Figure 1 the physically measured thickness of the shear band is 3 mm. Note that the angle of orientation is about 40^o to the vertical in the upper left corner. The shear band inclination gently increases as we move into the sample to 53^o at the central part of the specimen.

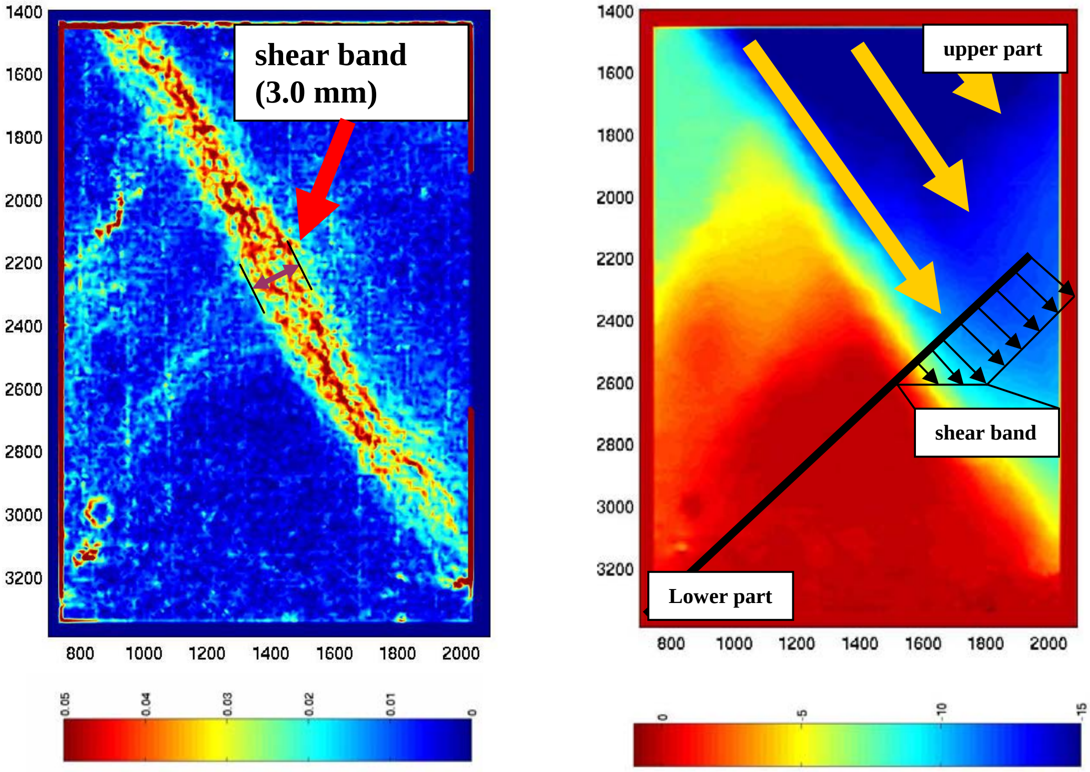

Figure 2. Incremental shear strain (left) and total displacement (right) plot at 581-583 (Courtesy; Dr. Steve Hall, 2006, L3S, Grenoble)

The situation “at the onset of localization” around the peak (581-583) is examined in further detail using a more refined PIV analyses and presented in Figure 2. Incremental shear strain plot (left) represents the kinematics of a localized deforming body and reveals the shear band thickness. A total displacement plot (right) illustrates that the specimen is splitted into three parts; the upper left part is moving downwards (showed with the arrows) while the lower part is attached to the fix bottom plate (of biaxial apparatus). In between the upper and the lower part there is an embedded shear band. The velocity of the moving block i.e. the upper part (an intact body), remains constant while the velocity decreases in the shear band to zero along the non-moving block below. Thakur et al (2006) provides additional information on the experimental work.

The experiments presented above suggest that when Norwegian quick clays fail they may do so along a finite shear band with a nonzero thickness. This is a very interesting observation, that supports the work by Jostad and Thakur (2006), showing similar features in a numerical study.

Finite element simulation of shear band

Jostad and Thakur (2006) suggest that the nonzero shear band thickness may be caused by an interaction of porewater flow and structural collapse. Herein, this idea is adopted and studied further by numerically simulating a displacement rate controlled biaxial test. The simulations are carried out using the Hardening Soil model available in finite element code Plaxis.

Strain localization is related to a decrease in shear resistance with increasing strain from a peak value to an ultimate or residual value. Simulating strain localization in quick clays by simple elasto plastic theory alone will not give good results. It is mathematically well proven that the finite element simulation of strain softening materials suffer from mesh dependency. This implies that the shear band thickness and its orientation is mesh dependent and the shear band thickness reduces to a value determined by the elements used, often the shear band will be one element wide.

In order to obtain a mesh independent physical thickness of shear band various methods, called regularization techniques, have been developed over the past couple of decades. In this study, a coupled formulation with pore water flow and a hardening elasto plastic constitutive relationship is used as a regularization method.
Since quick clay is a contracting material (negative dilatancy) positive excess pore pressure will develop inside the shear band (due to incompressibility of water). Even under globally undrained conditions porewater in the shear band will dissipate to the neighbouring body. The amount of local drainage in the shear band depends on strain rate and permeability of the material. Pore water flow out of the band will reduce excess porewater pressure in the shear band and hence the softening in the shear band.

Table 1 Input parameters

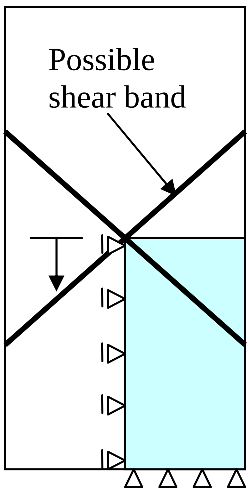

Figure 3. Model

Input	**unit**	**Value**		**Input**	**unit**	**value**
k_x	[m/day]	1E-6		ϕ	[°]	30
k_y	[m/day]	1E-6		ψ	[°]	-5
E_{50}^{ref}	kPa	60		ν	[-]	0.2
E_{oed}^{ref}	kPa	21.8		p_{ref}	kPa	1
E_{ur}^{ref}	kPa	211		Power	[-]	1
c_{ref}	kPa	5		K0nc	[-]	0.5
k_x	Permeability in x direction			ϕ	Friction angle	
k_y	Permeability in y direction			ψ	Dilatancy angle	
E_{50}^{ref}	Secant stiffness			ν	Poisson's ratio	
E_{oed}^{ref}	Tangent stiffness for primary oedometer loading			p_{ref}	Reference pressure	
E_{ur}^{ref}	Loading reloading modulus			Power	Power stress level dependent stiffness	
c_{ref}	Effective cohesion			K0nc	Ko for NC clays	

Since narrow shear bands drain faster than wider shear bands there will be a situation when internal drainage balances the tendency of softening and a steady state situation may develop. In such a situation, a unique shear band thickness can be expected (Jostad et. al 2006, Thakur 2006, Thakur et al. 2005). Motivated by the experimental study described above, a biaxial test is imitated using the Hardening Soil model available in the finite element code, Plaxis. The FE model of the sample is presented in Figure 3. Only a quarter of total specimen size is simulated due to symmetry. Table 1 gives a set of material parameters used for the soft sensitive clay i.e. quick clay.

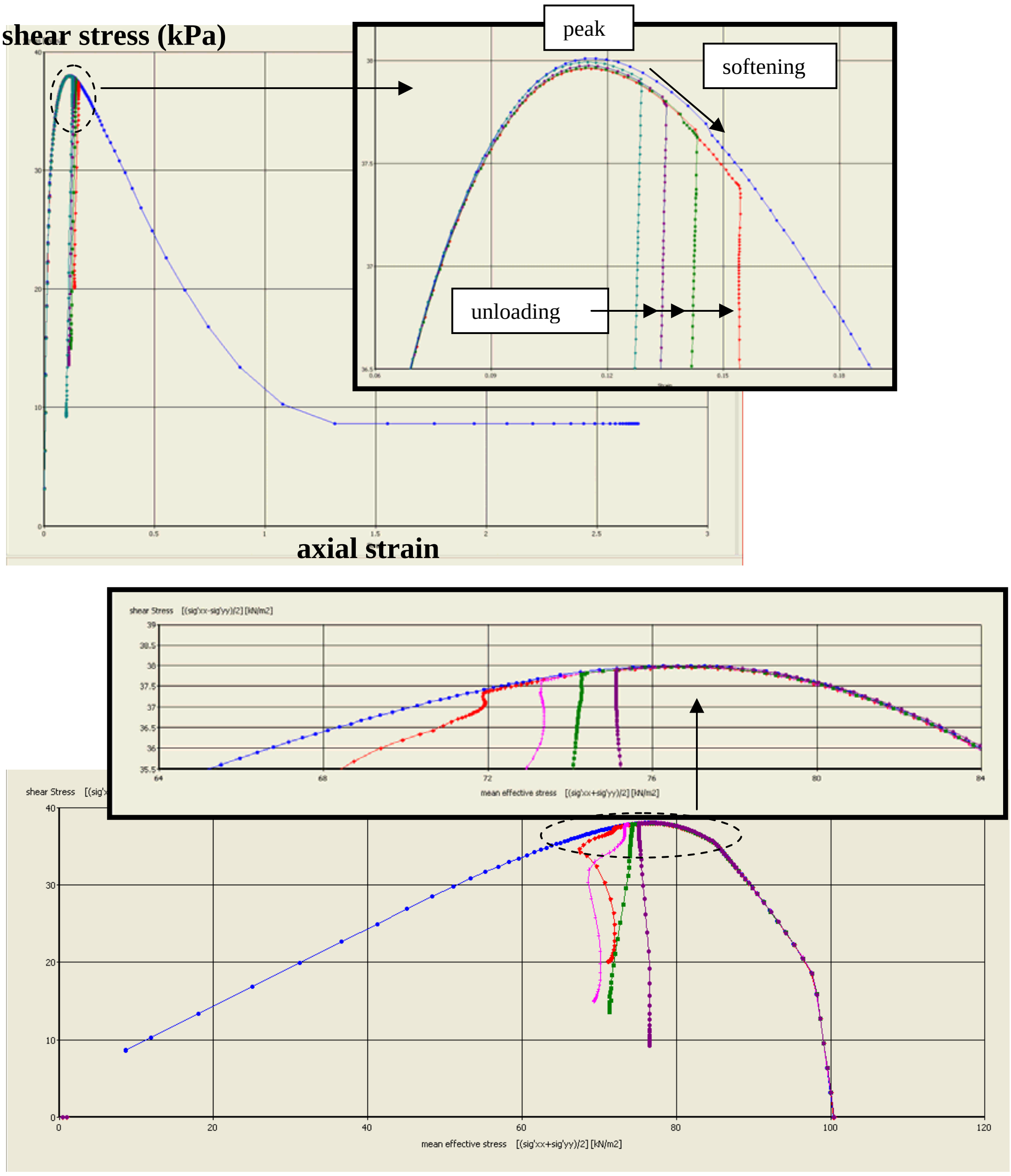

Figure 4. Local shear stress-effective mean stress-axial strain response for the individual material point

A strain rate of 6%/min is used in present study. Two different analyses are performed; with and without embedded weak element. Localization is observed in both cases however, in later case emergence of localization is not always guaranteed. Figure 4 shows a local stress strain response of individual material points (each curve represents one material point).

A material point that lies inside the shear band continues to soften, and the material point situated on the outside of the shear band follows the unloading path. Table 2 presents shear bands at different strain levels in order to visualize the different stages of localization during softening.

Table 2 summary of contracting shear band observed numerically

(1) ε_{yy} = 12.9% (axial strain)		**(2) ε_{yy} = 13.5% (axial strain)**	
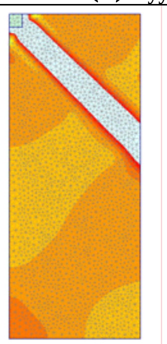 *Tsb = 5 element size = 2.50 mm (bigger than the size of the pertur-bation!)	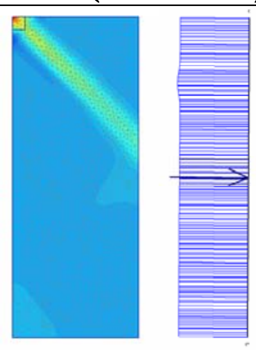 **pore pressure plot** max pp = 64.30kN/m^2	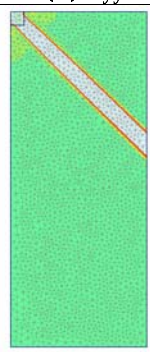 *Tsb = 3 element size = 1.5 mm (size of the purtur-bation)	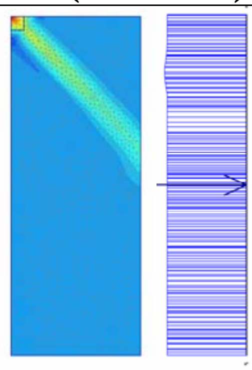 **pore pressure plot** max pp = 64.30kN/m^2
(3) ε_{yy} = 14.3% (axial strain)		**(4) ε_{yy} = 15.4% (axial strain)**	
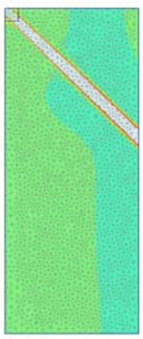 *Tsb = 2 elements size = 1.00 mm	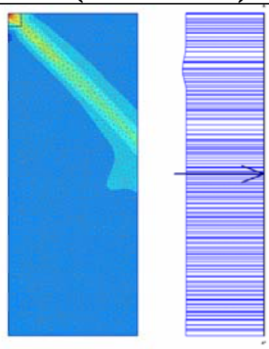 **pore pressure plot** max pp = 67.30kN/m^2	 *Tsb = 2 elements size = 1.00 mm	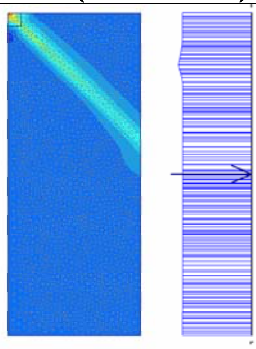 **pore pressure plot** max pp = 73.30kN/m^2

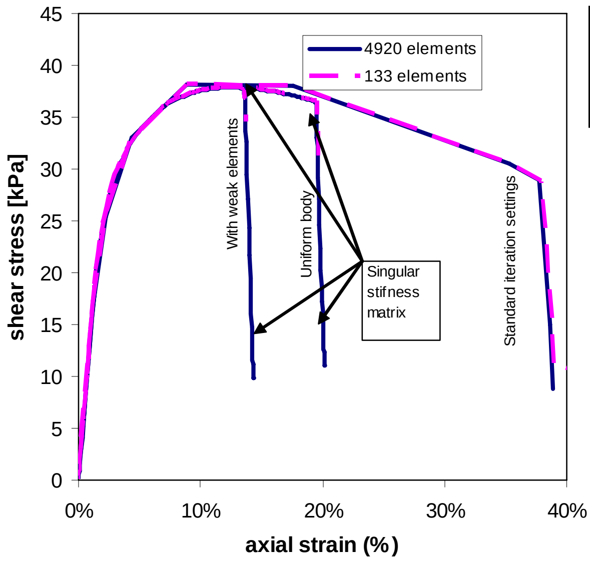

*Tsb = shear band thickness

Figure 5. Global response: shear stress versus axial strain

Table 2 shows that the shear band thickness is not unique and changes (decreasing) with the increasing local strain and ultimately goes to one element size. A global response of the model is shown in Figure 5. Elaborated discussion is presented in the following.

Finite element modelling of progressive failure in a quick clay slope

Usually slope stability analyses in FE is done either using dilatancy angle zero (non contracting behaviour and elastic perfectly plastic situation) even for a soft clays that has a negative dilatancy angle. The reason is to avoid mesh dependency. By doing so we ignore progressive failure as well.

In this section, one simple slope stability analyses is performed using the same parameters, as shown in Table 1. Stability analyses is performed using two different mesh sizes, however results are plotted only for the finer mesh. A complete discussion is provided in the next section.

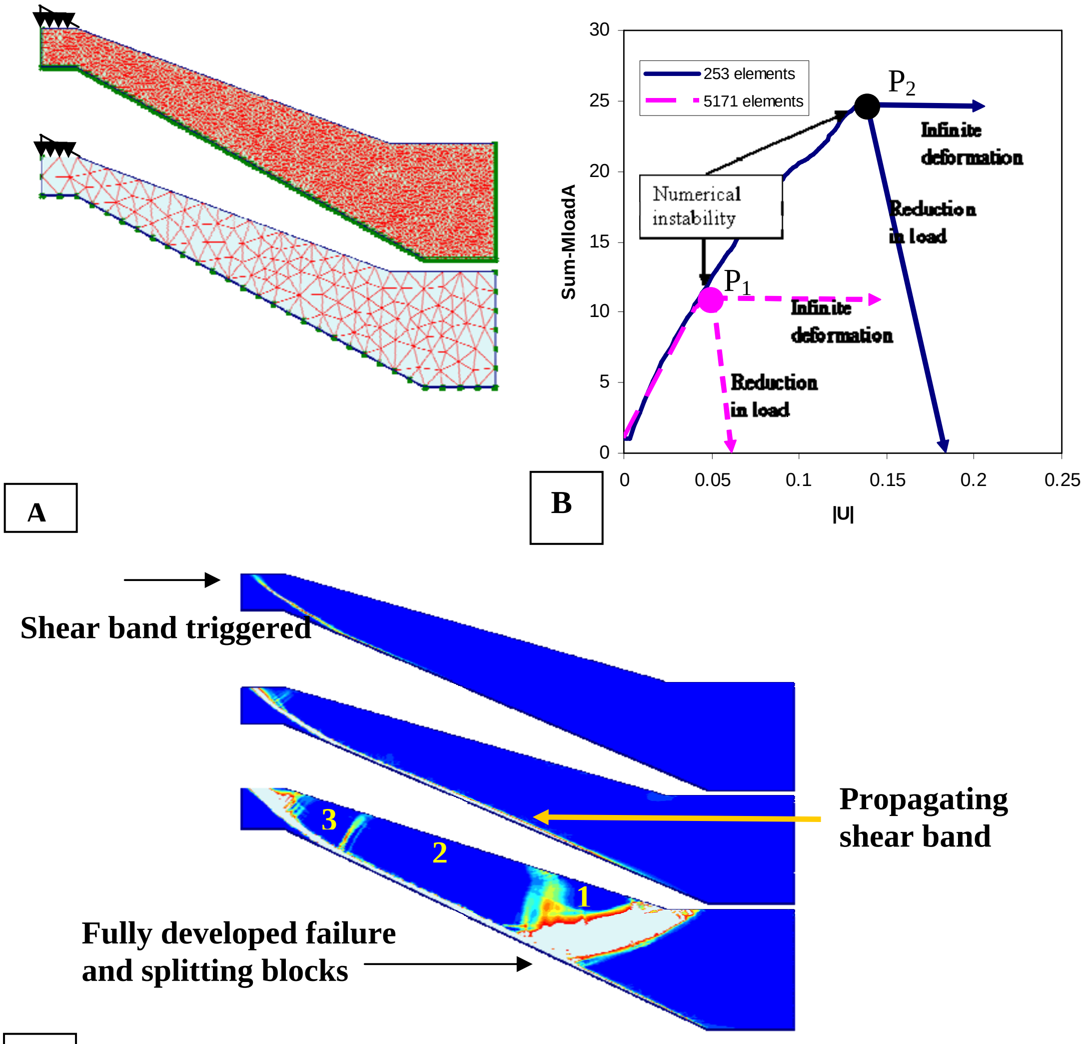

Figure 6. progressive failure in a long natural slope

Discussions

Based on analyses performed in earlier sections, the following discussion can be made;

(A) results obtained from experimental plane strain biaxial tests conducted in Norwegian quick clay depicts a distinct shear band thickness of 3.0 mm. However, undrained shear banding is not guaranteed for every strain rate.

(B) a biaxial specimen (refer Figure 3) that has a similar material property as of quick clays is numerically simulated to demonstrate the coupled pore water flow analyses that helps in regularizing strain localization type problem. A distinct shear band thickness is found at the onset of localization (at the peak shear stress or in post peak regime). Also, a unique global response can be obtained irrespective of element size (refer Figure 5). Note that finally the shear band reduces to one element size (Table 2), and in this situation the calculation stops due to numerical instability (as shown in Figure 5). In other words, this type of regularization technique has a limited scope, especially when using a rate independent elasto plastic platform (present study).

(C) Figure 4 represents a local stress strain characteristics of a numerically simulated biaxial specimen. In displacement rate controlled test biaxial test where shear stresses are uniform along the height of specimen, we may reach a peak shear stress before we fully mobilize the friction. This is caused by the non-associated flow rule. Hence a delayed localization emerges in post peak region once the friction is fully mobilized. In other words, apparently there can be two bifurcation points in stress strain curve, first at the peak where material decides whether or not to soften and the second in the post peak region where once again material has to decide either to develop a shear band (localized failure) or deform uniformly (diffuse failure).

(D) two different sizes of elements have been chosen for the biaxial simulation. Three different models were simulated; with imperfection, without imperfection and a simulation with an imperfection and large calculation steps (standard setting in Plaxis), refer Figure 4. All these cases give results independent of the mesh size. However, calculation stops once the shear band reduces to one element size due to a singular stiffness matrix. Calculation terminates much faster in case of the coarser mesh (2.74 mm) compare to the finer mesh (0.5 mm size). However, accumulated plastic strain within shear band remain same for both the cases. It is important to mention that analyses are somewhat sensitive to the iteration steps, higher step sizes shows a big jumps in stresses and strain while small step size helps to obtain a smooth transition. In this paper, only results using a fine mesh are presented.

(E) A comparison between laboratory biaxial plain strain test and FE is done;

1) In laboratory shear a band is observed for a global strain rate of 0.36%/hr, however no localization is obtained in finite element calculation for this rate i.e. numerically the specimen behaved as a locally drained material. So, a faster rate of 6%/min is used to simulate a localization.

2) Experimentally an ultimate thickness of shear band is observed (3.0 mm) while numerically a maximum thickness of shear band observed was equal to 2.5mm (perturbation size = 1.5 mm), but finally numerically shear band reduces to zero thickness. In other words, present study is valid until the localization emerges (giving a maximum shear band thickness). It is interesting to note that the maximum shear band thickness observed without any perturbation is also equal to 2.5mm.

   Orientation of the shear band is changing in the experiment, possibly due to restriction in horizontal movement of specimen while numerically (free movement in horizontal direction) the orientation of shear band is around 45 degrees.

3) Pre peak localization was observed experimentally, however it is not possible numerically for an isotropic and homogeneously deforming material.

(F) The use of coupled pore water regularization is not able to control (completely) the progressively failing slope. Explanation can be as; preliminary biaxial test results shows a specific thickness of shear band corresponds to a specific local stress strain characteristics for a given rate. Hence shear band thickness would be different along the progressively failing slope (due to changing stress strain state along the slope), and it reduces to a nil value (less than or equal to one element size) meaning that the local strains are extremely high.. In absence of any rate dependent parameter (artificial hardening, for instance viscosity etc.) coupled pore water and strain localization is not able to restrain shear band thickness to more than one element size. In figure 6 (B) represent a characteristic plot when numerical instability occurs; either force drops instantaneously or deformations increases to infinity without any decrease in forces. In reality none of the two. P_1 and P_2 represent points beyond which non-unique response may occur. To avoid such situation and to obtain a physical shear band thickness, a rate dependent modelling is encouraged.

An analogous model for the progressive failure is represented in Figure 7, a series of blocks are connected with the springs. If spring is rigid, then there is no progressive failure as all spring might reach to yielding together and share the equal stresses i.e. catastrophic failure. While soft spring may cause progressive failure where springs might yield one by one due transferred block weight from one to another at any time, the stress state of each spring is also plotted in Figure 7.

(G) Progressive failure in a soft sensitive clay slope is simulated. Localization triggers at the top of the slope and progressed towards the toe and finally a full growth of shear band along the slope is seen (refer figure 6 (C)). Moreover, once the failure is fully developed the slope tends to split in wedges (especially near to toe). Large deformations may develop retrogressively as commonly reported in the field.

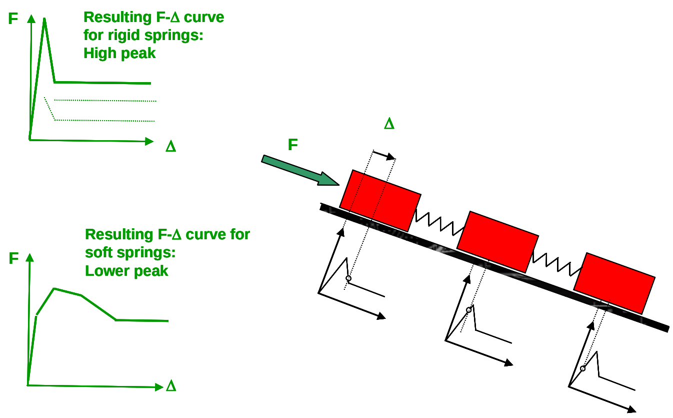

Figure 7. progressive failure mechanism (Nordal, 2004)

Conclusions

Based on the present study, the following conclusions are made;

(a) It is experimentally observed that in our particular test the quick clay has a distinct shear band thickness of 3 mm, however, it seems to be rate dependent.

(b) Displacement rate controlled coupled pore water flow type biaxial test have been carried out. For a specific global rate, mesh independent results has been observed. However, shear band thickness itself is rate dependent. In the absence of rate independent parameter within the hardening soil model in Plaxis, we are not able to control the softening rate and eventually we end up with a numerical instable situation.

(c) Using the same material model and parameter sets, progressive type failing slope is simulated. Once again, the rate independent constitutive model is not able to adjust with coupled flow formulations due to an excessive increase in strain in an very small zero time increment (strain rate tend to infinity). The calculation turn out to be undrained and mesh dependency results. In short, to obtain a distinct shear band and a unique result, a rate dependent material law must be utilized.

Recently a study is initiated by Jostad et al (2006) to capture strain localization in soft sensitive clays using rate dependent model. Here mesh independent and strain rate dependent shear band thickness is reported.

ACKNOWLEDGEMENTS: International Centre for Geohazards, NTNU-Geoteknikk and L3S, Grenoble is acknowledged for their financial and technical supports, respectively.

References

1. Desrues J. (1984). “La localisation de la déformation dans les matériaux granulaires.” *Thèse de Doctorat eScience*, USMG & INPG, Grenoble, France.

2. Drescher A., Vardoulakis I., Han C. (1990). “A biaxial apparatus for testing soils.” *Geotechnical Testing Journal, ASTM,* vol.13:3, pp. 226-234.

3. Hammad W. (1991) “Modélisation non linéaire et étude expérimentale des bandes de cisaillement dans les sables.” *Thèse de Doctorat de l'Université J. Fourier*, Grenoble, France.

4. Jostad H. P., Andresen L. and Thakur V. (2006) ”shear band thickness calculation in sensitive clays.” *6th European Conference on Numerical methods in Geotechnical Engineering,* NUMGE, Austria.

5. Nordal S. (2004) “Geohazards: Major Challenges” *XVI NGM Nordic Geotechnical meeting*, pp 65-81.

6. Thakur V, Nordal S., Jostad H. P. and Andresen L. (2005) “Study of pore water pressure dissipation during shear banding in sensitive clays.” *11th IACMAG, Volume*. 4 pp. 289-296.

7. Thakur V. (2006) “Shear band analyses in sensitive clays indicating inherent regularization.” *17th European young geotechnical conference,* Croatia.

8. Thakur V., Nordal S., Viggiani G. and Charrier P. (2006) “Coupled pore water flow and strain localization in soft sensitive clays: Experimental investigation” *International Journal of Acta Geotechnica* (in pipe line).

9. Vardoulakis I., Goldscheider M. (1981). “Biaxial apparatus for testing shear bands in soils.” *Proceedings, 10th ICSMFE, Stockholm*, 1981, 4/61, Balkema, Rotterdam, pp.819-824.